On the dynamic response of a pitch/torque controlled wind turbine in a pulsating dynamic wake

On the dynamic response of a pitch/torque controlled wind turbine in a pulsating dynamic wake

S Cacciola, A Bertozzi, L Sartori, A Croce

Dept. of Aerospace Science and Technology, Politecnico di Milano, via La Masa 34, 20156 Milano, Italy

E-mail: alessandro.croce@polimi.it

Abstract. The interaction between wakes and rotors is typically detrimental in terms of the overall power production of a wind farm. The recently studied wind farm controllers represent a promising way to increase the energy harvested through the mitigation of the effects induced by wake impingement. Recently, a novel methodology, based on a dynamic variation of induction, has been proposed as an alternative to steady induction and wake redirection controls. According to this new technology, a periodic collective motion of blade pitch generates a dynamic induction, associated with a stronger flow mixing and therefore a faster wake recovery. Although this technique proved to be effective in terms of power increase, both in numerical simulations and in wind tunnel experiments, much is to be done in order to demonstrate its feasibility. In particular, the impact of dynamic induction control in terms of downstream turbine dynamics has not been yet analyzed in detail. This paper presents a CFD-based analysis aimed at describing the response of a downstream rotor inside the wake of an upstream machine performing dynamic induction control. Specifically, the periodic induction entails a pulsating flow downstream which interacts significantly with the aero-servo-elastic dynamics of the downstream turbines. For low wind speeds, such an oscillating flow may trigger a shut-down/start-up sequence any time the velocity results lower than the cut-in speed.

1. Introduction

Wind farm control represents a promising way to increase the energy harvested by a wind farm. According to this technology, the operative conditions of the upstream turbines are modified so as to reduce the interaction between their wakes and the downstream machines. A wind farm control can be based on static induction control (SIC), which consists in reducing the power of the machine so as to increase in-wake flow velocity [1], and on wake redirection (WR), which promotes a redirection of the wake out of the downstream rotors by yawing the upstream machines [2].

Recently, a novel promising method, called dynamic induction control (DIC), has been proposed as an alternative to the aforementioned techniques. DIC method is based on a dynamic periodic variation of the axial induction, obtained by a rotor thrust modulation. Such a modulation can be effectively generated by a periodic collective motion (PCM) of the pitch of the blades. Through a complex interaction among blade tip vortices, in-wake flow and undisturbed wind, the PCM technique realizes an increased level of air mixing inside the wake. The wake itself eventually recovers faster. Potentially, a wind turbine, which finds itself inside such wake, experiences a higher mean flow velocity.

Dynamic induction control was firstly proposed and studied in [3] and [4] through CFD simulations based on actuator disk model. The first wind tunnel verification of DIC was presented in [5] along with a first analysis of the related impact in terms of fatigue of the upstream turbine, i.e. the one which generates the dynamic induction. Finally, in [6], the impact of this control at turbine level was analyzed through a rotor redesign process, including an analysis of the ultimate loads and of the maximum blade tip deflection.

From the studies conducted in [5, 4, 3], it was possible to assess that PCM is a valuable technique to increase the overall power production of a wind farm. Moreover, its effectiveness resulted significantly dependent on the amplitude and frequency of the pitch oscillation. In general, the frequency range in which one should find the optimal performance is associated to a Strouhal number between 0.15 and 0.5, being the Strouhal number a dimensionless value obtained multiplying the oscillation frequency by the ratio between rotor diameter and undisturbed wind speed.

Additionally, through multibody simulations [6], it was possible to evaluate the impact of PCM on the loading of the upstream turbine, which turned out to limited and comparable to the one related to wake-redirection-based control, for small amplitude of the pitch oscillation, e.g. about 2 deg.

What is however missing in the current status of the literature is a thorough analysis of the dynamic behavior of downstream turbines, i.e. the ones which feel the effect of DIC. In fact, varying periodically the induction of an upstream turbine also entails a periodic variation of in-wake velocity, along with an increase in its mean value. Hence, the downstream flow results pulsating and characterized by a velocity which significantly oscillates at the PCM frequency. Such a pulsating wake may first increase the fatigue loading of downstream machines, and, since farm controls are typically active in the below rated-speed region, may trigger a shut-down/start-up sequence any time the flow velocity results lower than the cut-in speed.

An analysis of the turbine and farm steady performances (e.g. mean total power) may therefore overlook some undesired effects due to the particular dynamical characteristics of resulting flow.

2. Objectives

The present paper aims at studying the effects of DIC based on PCM on the aero-servo-elastic response of a downstream turbine, which is located within a pulsating wake. Such a study requires high fidelity CFD-based simulations coupled with an aero-servo-elastic model of the wind turbines, in order to suitably evaluate the downstream turbine performance.

To the best Authors' knowledge, this work represents the first attempt to analyze dynamic induction control in terms of the aeroelastic response of a downstream turbine in a CFD environment.

To do so, after an explanation of the employed methodology in Sec 3, the paper deals with two sets of CFD-based analyses, in Sec. 4. In the first set, a study of the wake shed by a rotor operating with PCM is conducted, providing the evidence of the pulsating behavior of the wake itself. In the second set, several CFD simulations of a two-turbine farm subject to steady wind at 6.5 m/s and 9 m/s has been performed with the goal of evaluating the aero-servo-elastic behavior of the downstream turbine.

3. Methodology

The CFD-based tool chosen in this work is `SOWFA` (Simulator fOr Wind Farm Applications) [7], a software based on the incompressible solver of `OpenFOAM`, which implements a Large Eddy Simulation scheme (LES). `SOWFA` is linked with the aero-servo-elastic solver `FAST` [8], to model the presence of the flexible turbines. Both tools have been installed on the `MARCONI` high performance

computer, managed by the SCAI (SuperComputing Applications and Innovation) department of the Italian inter-university consortium CINECA.

The analyses of this work have been conducted on the well-known 5MW NREL reference wind turbine [9], whose FAST model was included in the CFD environment. The wind turbine model has a diameter D equal to 126 m and a rated wind speed equal to 11.4 m/s. A pretty wide region I-1/2 extends from the cut-in speed equal to 3 m/s to about 8 m/s. This model has been chosen here because it is representative of modern onshore wind turbines.

The reference control system of the 5MW NREL turbine, which is a standard pitch/torque controller based on PID, has been modified to include the sinusoidal PCM blade motion as

$$\beta_{\text{coll}} = \beta_{\text{trim}} + \beta_{\text{PCM}} \sin(2\pi\, f_{\text{PCM}}\, t + \phi_{\text{PCM}}), \tag{1}$$

where β_{coll} is the blade collective pitch setting, β_{trim} is the pitch angle imposed by the trimmer (i.e. the standard pitch-torque turbine regulator), t is the simulation time, whereas β_{PCM} and f_{PCM} are, respectively, the amplitude and the frequency set for PCM. Finally, ϕ_{PCM} is the phase of PCM oscillation, used to avoid discontinuity in blade pitch demand at the instant of PCM activation.

The PCM frequency is typically expressed through the dimensionless Strouhal number defined as

$$S_t = \frac{f_{PCM} D}{U_\infty}, \tag{2}$$

where U_∞ is the undisturbed wind speed.

4. Results

In this section, the results of two series of CFD simulations will be shown. At first, the flow downstream a rotor operating with and without PCM will be analyzed with the main goal of comprehending the characteristics of the flow itself and the impact it would have on a possible downstream machine, in the case of a stationary wind at 6.5 m/s. Then, in the second set of simulations, a simple two-turbine farm subject to a stationary wind at 6.5 and 9 m/s will be considered, with the final aim of evaluating the aero-servo-elastic dynamic response of the downstream machine. The 6.5 and 9 m/s values have been chosen as they are in the middle of region I-1/2 and II, respectively. This also makes it possible to assess the impact of PCM in the different regions of operation ([9]).

Clearly, the analyses are all performed for stationary winds in order to ease, in a preliminary stage of this research, the evaluation of the effects of PCM, which in turbulent conditions would result masked under turbulence-induced flow fluctuation. Moreover, even though the turbulence may affect the results significantly, the analysis present in this paper can be viewed also as an approximation for very low turbulence intensity cases. The more complex case with a realistic atmospheric boundary layer is, hence, out of the scope of this paper, and is being currently analyzed by the Authors and the results will be made available in future publications.

4.1. Effect of PCM on the flow downstream a single turbine

For this first sets of simulations, which consider only a single wind turbine, a cuboid domain with dimensions equal to $10 \times 10 \times 15\,D$ has been considered. The wind blows towards the longest dimension whereas the turbine is located in the center-line at a distance of $5D$ from the inlet face. The separation between the turbine and the domain faces allows the wake to develop avoiding numerical problems that could arise closed to the domain boundaries.

Four levels of circular refinements around the rotor center have been considered to have a better modeling of the flow where rotor and wakes are present. The final mesh has 6'237'760 hexahedral and 116'576 polyhedral cells, with a size of about 2 m in the most refined parts and 31.5 m in the outer regions.

A Dirichlet condition, corresponding to a constant wind at 6.5 m/s, is set to the inlet and the outlet boundaries, while standard periodic conditions are considered for the other domain faces.

The constant time step of `SOWFA` simulation was set equal to 0.048 seconds, whereas a step of 0.048/3=0.016 seconds was used for `FAST`, meaning that three substeps of the aeroelastic solver take place within a single step of CFD time marching. After a study on the impact of time step reduction on wake development, not shown here for the sake of brevity, the selected time steps resulted to be adequate to capture the relevant behavior of both aeroservoelasticity and fluid dynamics. With these settings, on `CINECA - MARCONI` platform, a simulation running for 800 seconds takes about 12 hours with 272 cores.

Four 800-second `SOWFA` simulations have been performed to evaluate the impact of the PCM on the wake. The first one was conducted without the wind farm controller, in order to define a reference case. In the other cases, the PCM was active and three different PCM frequencies has been considered. In particular, based on previous works presented in literature (see [4], [5] and [6]), we have considered Strouhal numbers of $S_t = 0.1, 0.3$ and 0.5, which correspond, for this case, to frequency values f_{PCM} equal to 0.0324, 0.0975 and 0.1625 rad/s, respectively. Again, from the literature cases (see [5, 6]), the amplitude β_{PCM} was fixed to 2.5 deg, a medium-high value which allows us to better highlight the PCM effects. The amplitude chosen for β_{PCM} represents a reasonable value within the range where optimal performance is expected, as suggested in [5].

Figure 1 shows the average flow velocity at a cross section located at $5D$ downstream. The four subplots refer to the reference case, i.e. without PCM, at up-left, and the cases with PCM for $S_t = 0.1, 0.3$ and 0.5, respectively at up-right, bottom-left and bottom-right. Since the PCM entails a periodic variation of the downstream flow velocity, the mean value of the flow speed $\bar{U}$ has been computed by averaging over a window equal to one PCM period, as

$$\bar{U}(x,y) = \frac{1}{T_{\mathrm{PCM}}} \int_{T_{\mathrm{PCM}}} U(x,y;t)\mathrm{d}t, \tag{3}$$

where x and y are the horizontal and vertical coordinates defining a cross-sectional plane, t is the time, U is the streamwise flow velocity and T_{PCM} is the PCM period corresponding to about 194, 64 and 39 seconds respectively for S_t =0.1, 0.3 and 0.5.

An increase of the in-wake flow velocity with respect to the reference case is clearly visible as a demonstration of the capability of PCM to promote a faster wake recovery.

In order to quantify this increment and try to infer its potential impact on the power produced by another downstream turbine, if it were inside the wake at $5D$, two different mean value definitions have been introduced. The standard arithmetic average as

$$\bar{U}_{\mathrm{arithmetic}} = \frac{1}{A_{\mathrm{rotor}}} \int_{A_{\mathrm{rotor}}} \bar{U}(x,y)\,\mathrm{d}A_{\mathrm{rotor}}, \tag{4}$$

and the cubic one, inspired by the fact that the power is proportional to the cube of the velocity, as

$$\bar{U}_{\mathrm{cubic}} = \left(\frac{1}{A_{\mathrm{rotor}}} \int_{A_{\mathrm{rotor}}} \bar{U}^3(x,y)\,\mathrm{d}A_{\mathrm{rotor}} \right)^{1/3}, \tag{5}$$

being A_{rotor} the rotor area and $\bar{U}(x,y)$ the averaged streamwise velocity computed as in (3).

Table 1 displays the increment of the mean streamwise velocity with respect to the case without PCM in terms of arithmetic and cubic averages for the three analyzed Strouhal numbers.

From the obtained results, it is possible to see, for all analyzed cases, an increase of about 30% of the in-wake flow velocity induced by PCM. This increment would entail a higher power extracted in a downstream turbine.

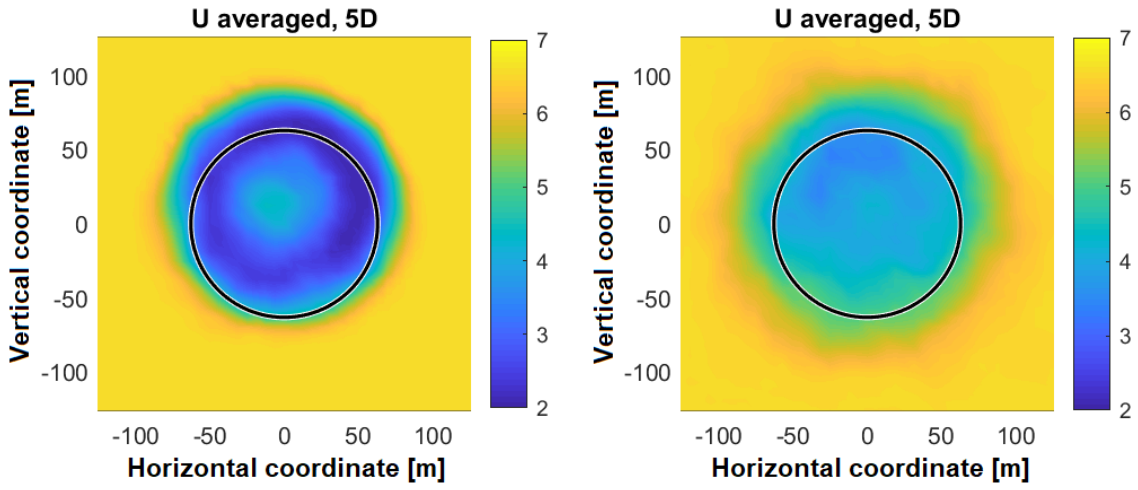

(a) Without PCM

(b) $S_t = 0.1$

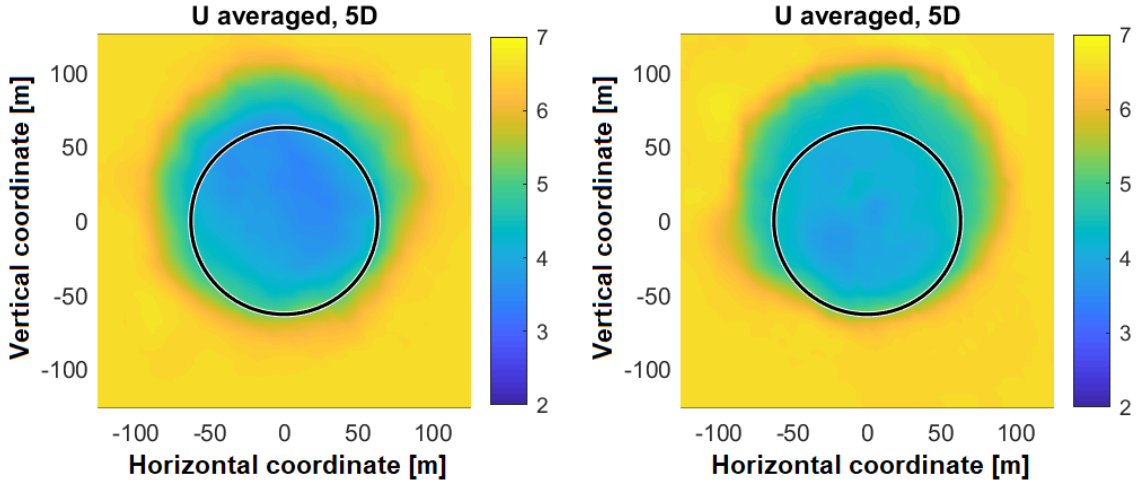

(c) $S_t = 0.3$

(d) $S_t = 0.5$

Figure 1: Averaged streamwise flow velocity $\bar{U}$ at $5D$ downstream. The black circle represents the position of the rotor.

Table 1: Arithmetic and cubic averaged flow velocities, in m/s, for different PCM Strouhal numbers at 5D downstream the rotor

	Arithmetic m/s (%)	Cubic m/s (%)
Reference	3.31	3.67
$S_t = 0.1$	4.31 (+30%)	4.39 (+20%)
$S_t = 0.3$	4.25 (+28%)	4.36 (+19%)
$S_t = 0.5$	4.45 (+34%)	4.53 (+23%)

This result is not surprising and, in one sense, represents a demonstration of the potential effectiveness of PCM already reported in literature. In fact, the Strouhal numbers considered in this investigation were selected in the range in which one may expect the best performance of PCM[5, 4].

However, beside its mean velocity, it is important to also analyze the time variability of the flow, which may impact on the dynamic response of a turbine inside the wake.

To this end, the mean flow velocity within the rotor disk, $U_{\text{rotor}}(t)$, has been computed for different sections downstream at each time step of the simulations as

$$U_{\text{rotor}}(t) = \frac{1}{A_{\text{rotor}}} \int_{A_{\text{rotor}}} U(x, y; t)\, \mathrm{d}A_{\text{rotor}}. \tag{6}$$

Figure 2 shows, for the case of $S_t = 0.1$ and uniform wind speed equal to 6.5 m/s, the time history of U_{rotor} at $4D$, $5D$, $6D$ and $7D$, which represent examples of possible turbine spacing of interest for present and future closely-spaced wind farms. The plot displays only the last two PCM periods of the simulations.

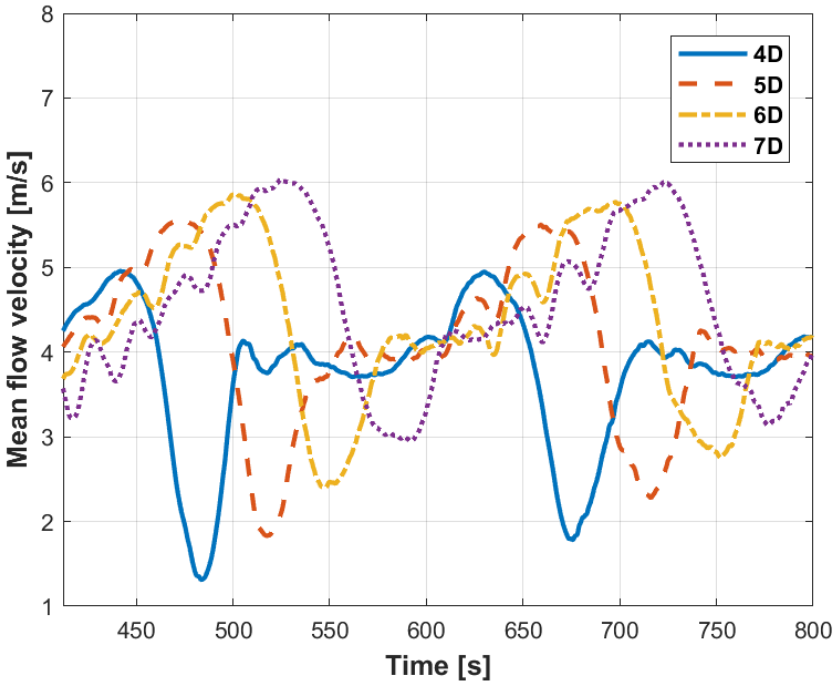

Figure 2: Averaged flow velocity as function of time at different downstream section. Uniform wind speed 6.5 m/s, PCM Strouhal 0.1.

Some comments can be done by looking at this plot. First of all, it is possible to note that the flow actually appears as if it were produced by a pulsating wake, as suggested by the oscillations at the PCM frequency, observed for all downstream distances. This behavior is expected to impact the closed-loop dynamic response of the downstream wind turbine operating in that pulsating wake. The time shift in the velocity peaks and holes at different downstream distances is due to the delay in the wake propagation. Moreover, the strength of wake pulsations decreases slightly, but still persists by moving away from the rotor. Finally, the mean value of the velocity increases with the distance as an effect of the standard wake recovery. These time histories show the particular characteristic of the wake induced by the PCM, which has inspired the

development of this work: the in-wake flow velocity, besides being higher on average, oscillates significantly at the PCM frequency and may drops to values lower than the cut-in speed (3 m/s). To this end, the dynamic response of a downstream turbine (in this case the aero-servo-elastic model) inside such a pulsating represents an interesting topic of investigation.

4.2. Analysis of two-turbine wind farm at 6.5 and 9 m/s

In order to asses the aero-servo-elastic behavior of a turbine inside a wake generated by an upstream machine operating with the PCM, a simple two-turbine wind farm has been considered. A second 5MW NREL reference wind turbine model [9] has been included $5D$ downstream. The computational domain has been coherently increased to a cuboid of dimensions $1260 \times 1260 \times 2646$ m, corresponding to $10 \times 10 \times 21\, D$. The two rotors are aligned to the wind direction and to the longest domain size.

As in the single turbine case, four local refinements ensure a mesh of good quality in the region where the turbines are located and where their wakes develop. The total number of cell is now grown to 9'062'504 of hexahedral and 167'528 of polyhedral types. Sizes of cells are similar to those obtained for the single turbine case presented in the previous Sec. 4.1.

On `CINECA - MARCONI` architecture, a simulation running for 800 seconds takes about 17 hours with 272 cores.

At first, the same stationary wind condition at 6.5 m/s, in the region I-1/2 for this machine, has been considered. Similarly to the case analyzed in Sec. 4.1, the first turbine generates a PCM with the same amplitude $\beta_{\mathrm{PCM}} = 2.5$ deg and three frequencies corresponding to Strouhal numbers equal to $S_t = 0.1$, 0.3 and 0.5.

Figure 3 shows, on the top, the time history of the flow velocity at the location of downstream turbine hub, and, on the bottom, the related power. As one can see, for the lowest Strouhal $S_t = 0.1$, red solid curve, the wind fluctuations in the wake are so high that the turbine shuts down for speeds lower than cut-in and starts up once the flow velocity gets higher. In fact, looking again at the same curve, after standard working condition (seconds 400–520), the turbine shuts down (seconds 520-540) and then starts up again (seconds 540-600). The succession of these three phases generates an undesired response of the downstream turbine. This has an important effect on the total wind farm power output and on its quality that must be included in the cost-benefit analysis related to the wind farm control synthesis. Of course, this issue could be, at least in part, mitigated with an ad hoc optimization of the start-up procedure, not considered here.

In Tab. 2, the mean power outputs associated to this farm configuration are reported. Increase of total power with respect to the case without PCM is up to 20%. Table 2 suggests also that significant gains can be achieved also for higher Strouhal numbers. However, the range $S_t > 0.5$ was intentionally not considered in the present investigation as it is also associated to higher impact on loads [6].

Another set of simulations has been conducted at 9 m/s, which belongs to the region II. Figure 4 shows the time histories of power outputs of the downstream machine for the reference case and three Strouhal numbers. Differently from what happened at 6.5 m/s, the downstream turbine does not shut down even for very low PCM Strouhal number. This behavior is simply explainable as the undisturbed wind speed is higher and, in turn, the in-wake velocity results higher as well. Nevertheless, the power quality becomes worse due to strong fluctuations. Finally, Tab. 3 reports the mean power produced by the entire wind farm. In this case, an increase up to the 15% can be observed.

5. Conclusions

This work presents a CFD-based study of the performances of a downstream turbine operating in a pulsating wake induced by an upstream machine performing a dynamic induction control

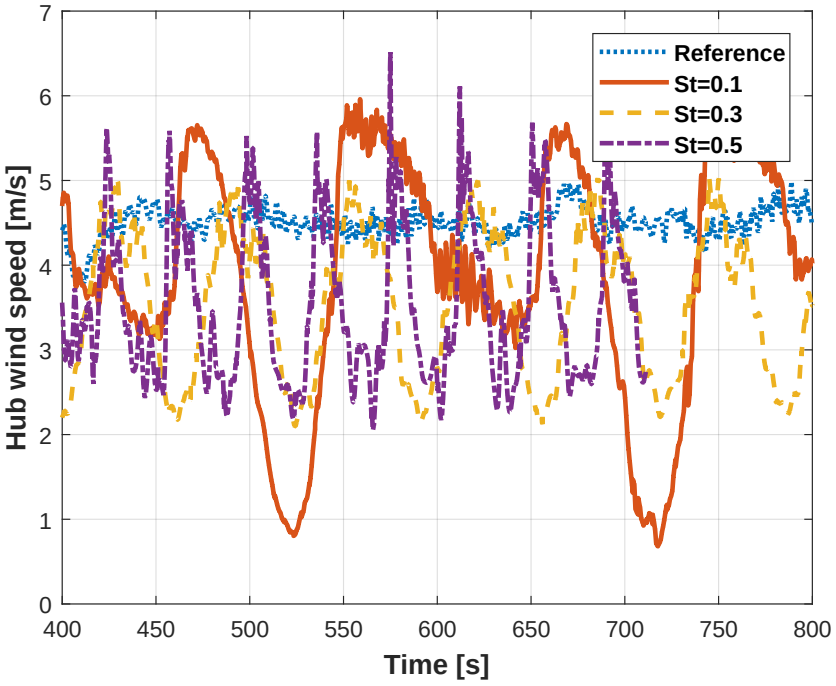

(a) Flow velocity at hub height of downstream turbine.

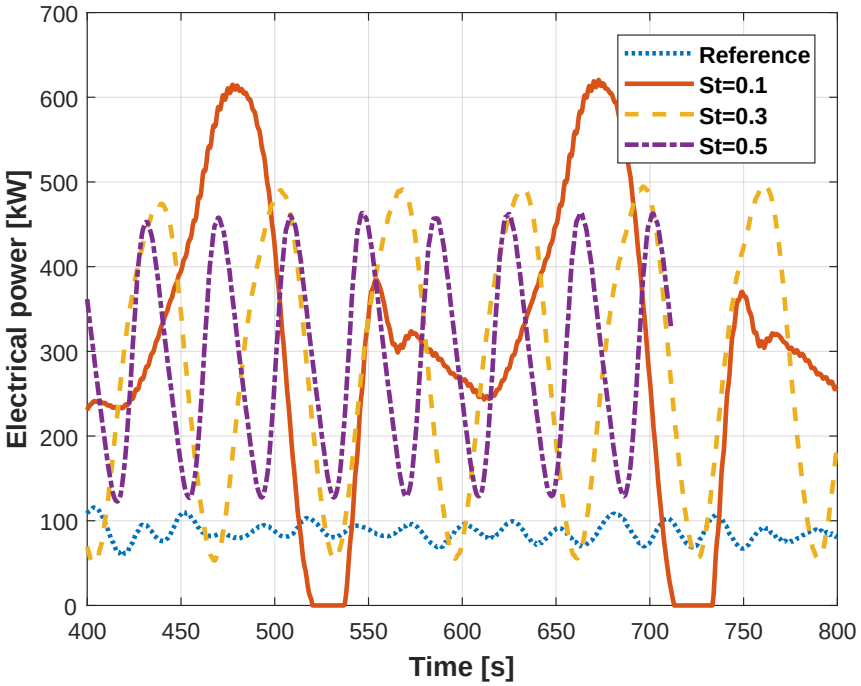

(b) Power generated by downstream turbine.

Figure 3: Effect of pulsating wake induced by DIC on the performance of a downstream turbine. Upper plot: flow velocity at hub height. Bottom plot: generated power.

Table 2: Power outputs, in kW, for the two-turbine wind farm without ("Reference") and with PCM at 6.5 m/s.

	Turbine #1 kW	Turbine #2 kW	Farm kW	Gain [%]
Reference	1053	87	1140	-
$S_t = 0.1$	1034	314	1348	18.2
$S_t = 0.3$	1061	290	1351	18.6
$S_t = 0.5$	1074	294	1367	20.0

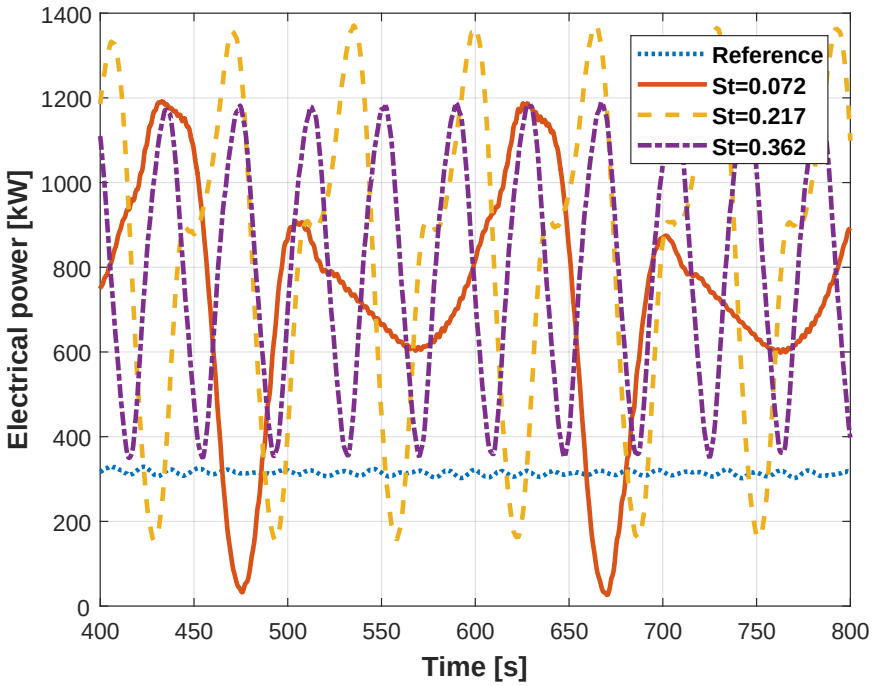

Figure 4: Power generated by downstream turbine. Undisturbed wind speed 9.0 m/s.

Table 3: Power outputs, in kW, for the two-turbine wind farm without (reference) and with PCM at 9.0 m/s.

	Turbine #1 kW	Turbine #2 kW	Farm kW	Gain [%]
Reference	2775	313	3088	-
$S_t = 0.072$	2780	721	3429	11.0
$S_t = 0.217$	2751	821	3573	15.7
$S_t = 0.362$	2774	797	3572	15.7

(DIC), through a periodic collective motion of pitch angle (PCM). At first, it has been demonstrated that the wake generated by a turbine operating with a PCM is pulsating, and hence is characterized by a higher mean value but also by important oscillations of flow velocity at the PCM frequency. Then, it has been shown that the pulsating wake may have detrimental effects on the downstream turbine dynamic response. In particular, for a wind of 6.5 m/s, it has been observed that the downstream machine may undergo shut-down/start-up sequences for very low wind velocity and low PCM frequency, with potential detrimental impact on the degradation of the turbine sub-components and on the power output quality. A similar analysis conducted for a uniform wind speed equal to 9 m/s showed that such shut-down/start-up sequences are not present.

Clearly, this work is only a preliminary step for a complete evaluation of the downstream turbine performance operating within a pulsating wake generated by the dynamic induction strategy. Many aspects are to be still investigated. For example, turbulence intensity may play a significant role in this scenario and deserves a special attention. In general, higher turbulence levels are associated to faster wake dissipation. Hence, we expect the impact of the dynamic induction control to decrease as the turbulence increases, as in the case with other wind farm control techniques, such as the wake redirection. A preliminary investigation in wind tunnel suggests that the dynamic induction control provides an increase in the total wind farm production even with non-negligible turbulence intensity [5]. Finally, also tower and nacelle modeling within the CFD environment should also be considered to have a more accurate assessment of the wake development.

All these important aspects are currently under investigation by the authors.

Acknowledgements

This work has been partially supported by the CL-Windcon project, which receives funding from the European Union Horizon 2020 research and innovation program under grand agreement No. 727477.

The Authors would like to thank Umberto Tettamanti, M.Sc., who provided the installation of `SOWFA` coupled with `Fast v.8` on `CINECA - MARCONI` computers.

We acknowledge the `CINECA` award under the ISCRA initiative, for the availability of high performance computing resources and support.

References

[1] Annoni J, Gebraad P M, Scholbrock A K, Fleming P and v Wingerden J W 2016 *Wind Energy* **19** 1135—1150
[2] Fleming P, King J, Dykes K, Simley E, Roadman J, Scholbrock A, Murphy P, Lundquist J K, Moriarty P, Fleming K, van Dam J, Bay C, Mudafort R, Lopez H, Skopek J, Scott M, Ryan B, Guernsey C and Brake D 2019 *Wind Energy Science* **4** 273–285 URL `https://www.wind-energ-sci.net/4/273/2019/`
[3] Munters W and Meyers G 2017 *Philosophical Transactions of the Royal Society A: Mathematical, Physical and Engineering Sciences* **375** 20160100–1–19
[4] Munters W and Meyers G 2018 *Wind Energy Science* **3** 409—-425
[5] Frederik J A, Weber R, Cacciola S, Campagnolo F, Croce A, Bottasso C and van Wingerden J W 2020 *Wind Energy Science* **5** 245–257 URL `https://www.wind-energ-sci.net/5/245/2020/`
[6] Croce A, Cacciola S, Sartori L and De Fidelibus P 2020 *Wind Energy Science Discussions* **2020** 1–26 URL `https://www.wind-energ-sci-discuss.net/wes-2019-103/`
[7] Churchfield M and Lee S 2012 Nwtc design codes-SOWFA Tech. rep. National Renewable Energy Laboratory (NREL) URL `http://wind.nrel.gov/designcodes/simulators/SOWFA`
[8] Jonkman J and Buhl Marshall L J 2005 Fast user's guide Tech. Rep. NREL/EL-500-38230 National Renewable Energy Laboratory (NREL)
[9] Jonkman J, Butterfield S, Musial W and Scott G 2009 Definition of a 5-mw reference wind turbine for offshore system development Tech. Rep. NREL/TP-500-38060 National Renewable Energy Laboratory (NREL)